Polarization-dependent encapsulated Dammann device under second Bragg illumination

ZHISEN HUANG[a], BO WANG [a,b,*], KUNHUA WEN[a], ZIMING MENG[a], ZHAOGANG NIE[a], FANGTENG ZHANG[a], XIANGJUN XING[a], LI CHEN[a], LIANG LEI[a], JINYUN ZHOU[a]
[a]*School of Physics and Optoelectronic Engineering, Guangdong University of Technology, Guangzhou 510006, China*
[b]*Guangdong Provincial Key Laboratory of Information Photonics Technology, Guangdong University of Technology, Guangzhou 510006, China*

A polarization-dependent beam-splitting encapsulated device under second Bragg angle is proposed. This grating device is mainly made of fused silica and silver plate, which can diffract the energy of TE-polarized light and TM-polarized light to 0th order and -2nd order, respectively, where the diffraction efficiency of both orders can reach 95% or more. In this design, a covering layer is introduced, which can improve the performance and protect the grating layer structure. For a given incident wavelength of 1550 nm and a period of 2962 nm, the rigorous coupled wave is used to optimize the thickness of the grating and the groove thickness of the grating. The results show that the polarization beam-splitting grating can be accurately designed with high efficiency and high extinction ratio, whose optical characteristics can be applied to the optical communication industry.

(Received September 1, 2020; accepted August 16, 2021)

Keywords: Beam splitting, Polarization dependence, Under second Bragg illumination

1. Introduction

Dammann gratings [1-6] have special diffraction characteristics that enable optical functions not possible with many conventional optics. Designed gratings can be as reflectors [7-9], combiner [10], phase retardation wave plates [11,12], filter [13-16], polarizers [17-20]. Polarization control is important for numerous optical systems [21-26]. And polarization beam splitters [27-30] made with gratings have many advantages over other conventional optical beam splitters. Sub-wavelength grating devices are easy to integrate and can process optical communication bands for dense wavelength multiplexing systems [31-34]. *Zheng et al*. designed the reflective polarizing beam splitter under the Bragg incidence by using the modal method and the rigorous coupled-wave method [35]. The efficiency of TE polarization is 98.5%, and the efficiency of TM polarization is 96.7%. *Wang et al.* present a novel metal-based phase grating for high-efficiency polarizing beam splitter. The efficiency of -1st order under TE polarization is 97.75%, and the efficiency of the 0th order is 96.90% under TM polarization [36]. As far as we know, no one has designed the polarization splitting of the reflection encapsulated grating with the incident wavelength of 1550 nm under second Bragg incidence. We designed a reflective polarization beam splitter, in which the efficiency of 0th order under TE polarization is 97.49%, and the efficiency of -2nd order under TM polarization is 95.65%.

The vector diffraction theory for designing micro-gratings mainly includes rigorous coupled-wave theory [37], modal method [38], finite element method and finite time domain difference method. The rigorous coupled-wave is mainly to solve the Maxwell's equations, and the diffraction efficiency of the reflected and transmitted light is obtained by combining the boundary conditions. However, the rigorous coupled-wave method can not explain the physical meaning of the grating in the reflection process. Therefore, the electric field distribution of the grating is given to obtain the energy distribution.

In this paper, a polarization-dependent beam-splitting grating with a connecting layer and covering layer under second Bragg incidence is reported. With a duty cycle of 0.6, a period of 2962 nm, and a connecting layer of 0.49 μm, rigorous coupled-wave is used to optimize the parameters of the grating. Compared with the beam-splitting grating under Bragg angle [35], the polarization-dependent grating in this paper can separate polarized beams into different directions.

2. Numerical rigorous optimization of polarization-dependent beam splitter

The structure of the sandwich-type polarization beam splitter under second Bragg incidence is shown in Fig. 1. After the incident light is incident on the grating, TE-polarized light is reflected to the 0th order, and TM-polarized light is reflected to the -2nd order, which achieves the polarization splitting effect. From top to bottom, the structure of the grating is divided into a covering layer, a grating layer with a connecting layer, Ag reflective layer and substrate. The period of the grating is d, the height and width of the grating ridge are h_2 and b, and the duty cycle f is b/d. The heights of the covering layer and the connecting layer are h_1 and h_3. The material of the covering layer and the grating ridge is fused silica with the refractive index of fused silica is n_2=1.45. The medium of the grating groove is air, where the refractive index of air is n_1=1.00. A beam of light enters the grating at the incident angle θ=sin^{-1}(λ/d). Ag has the advantage of strong plasticity, it is selected as the reflective layer of the grating with the refractive index of n_m = 0.469-9.32i.

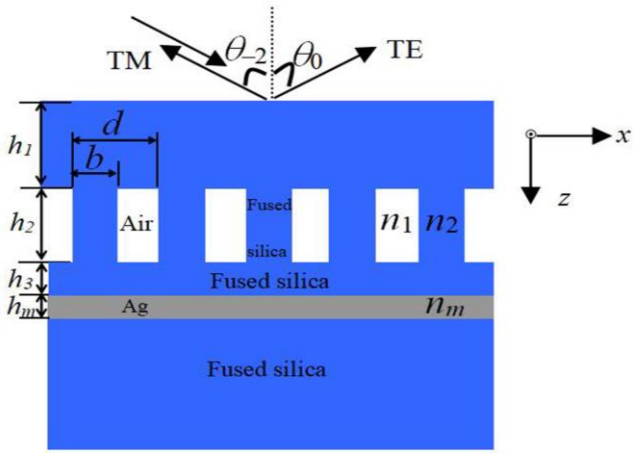

Fig. 1. The schematic diagram of the reflective polarization-dependent grating polarizer under second Bragg angle incidence (color online)

According to the rigorous coupled-wave method, the expressions of the electromagnetic fields in the incident region and the transmitted region can be given. Then, the Fourier series is used to expand the dielectric constant of each grating layer so as to derive the coupled wave equations. Finally, the boundary conditions are combined to solve the amplitude and diffraction efficiency of each order. The reflection efficiency is:

$$DE_{ri} = R_i R_i^* \,\mathrm{Re}\left[\frac{\sqrt{d^2-\lambda^2\left(\frac{1}{n_1}-i\right)^2}}{\sqrt{n_1^2 d^2-\lambda^2}}\right], \tag{1}$$

where R_i is the field amplitude. Therefore, the reflective property can be investigated by the RCWA method.

Fig. 2 shows the efficiency and extinction ratio versus the thicknesses of the covering layer and grating layer for two polarizations. The diffraction order includes the 0th order efficiency under TE polarization and the -2nd order under TM polarization. As can be seen in Fig. 2, the design optimization can be chosen as h_1 = 0.87 μm and h_2 = 1.96 μm. The efficiency of TE polarization is mainly concentrated on the 0th order, and the efficiency reaches 97.49%. The efficiency of TM polarization is mainly concentrated on the -2nd order, and the efficiency reaches 95.65%. At this time, the two orders of extinction ratio are 34.46 dB and 48.19 dB, respectively. The extinction ratio is greater than 20 dB, which meets the needs of general applications.

Based on the data in Fig. 2, the mode field distribution of the grating is analyzed. Fig. 3 shows the field distribution normalization of the polarization beam-splitting grating. Fig. 3(a) reflects the energy distribution of the grating in the 0th order under TE polarization, and Fig. 3(b) reflects the energy distribution of -2nd order under TM polarization. The incident light of 1550 nm is incident on the grating surface, passes through the grating region, and is reflected by the metal mirror, and passes through the grating region for the second time to obtain reflection efficiency.

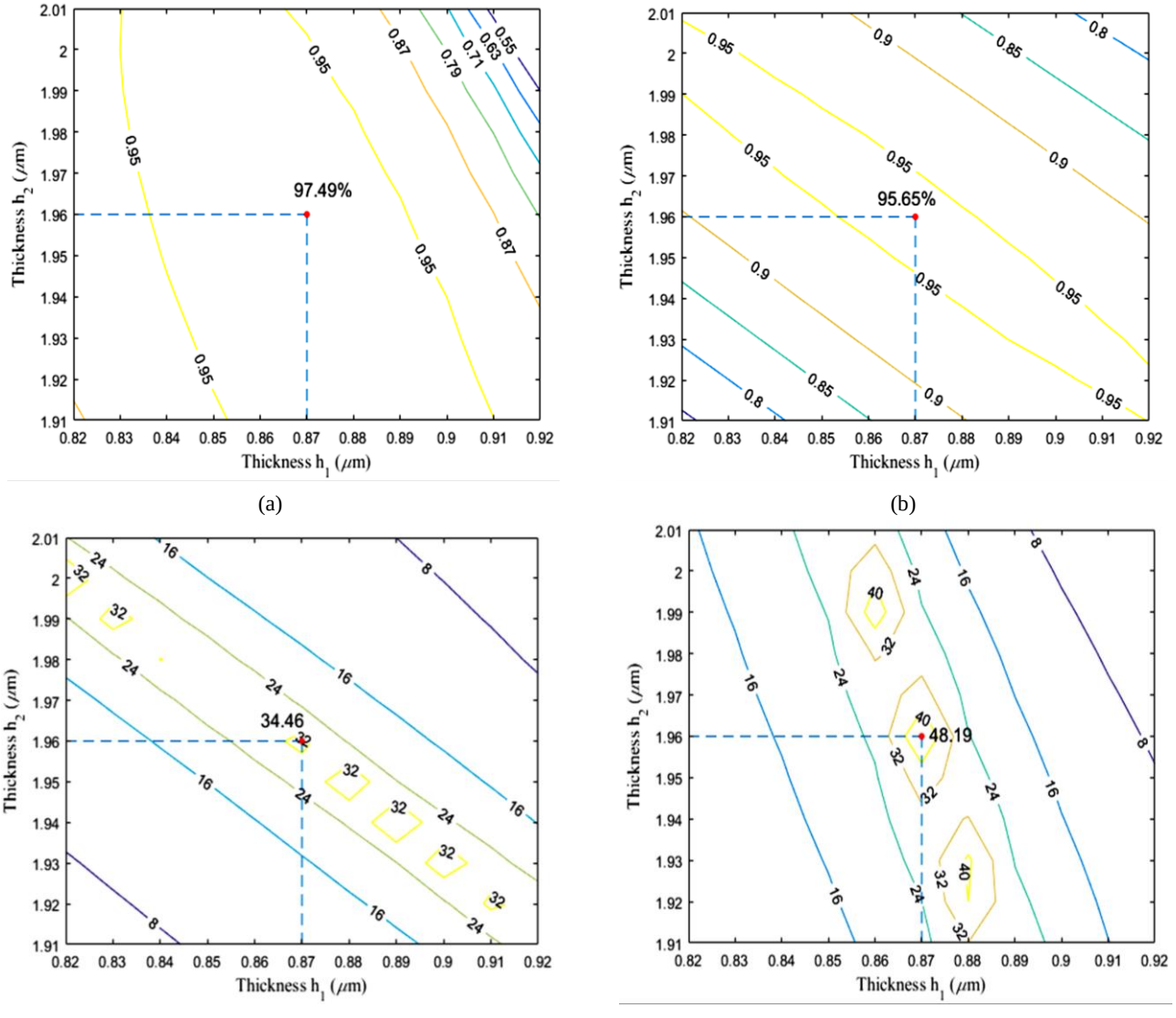

Fig. 2. Performance in two orders for the grating versus the thickness of two layers for both two polarizations at wavelength of 1550 nm under second Bragg angle incidence: (a) efficiency in 0th order for TE polarization, (b) efficiency in -2nd order for TM polarization, (c) extinction ratio in 0th order, (d) extinction ratio in -2nd order (color online)

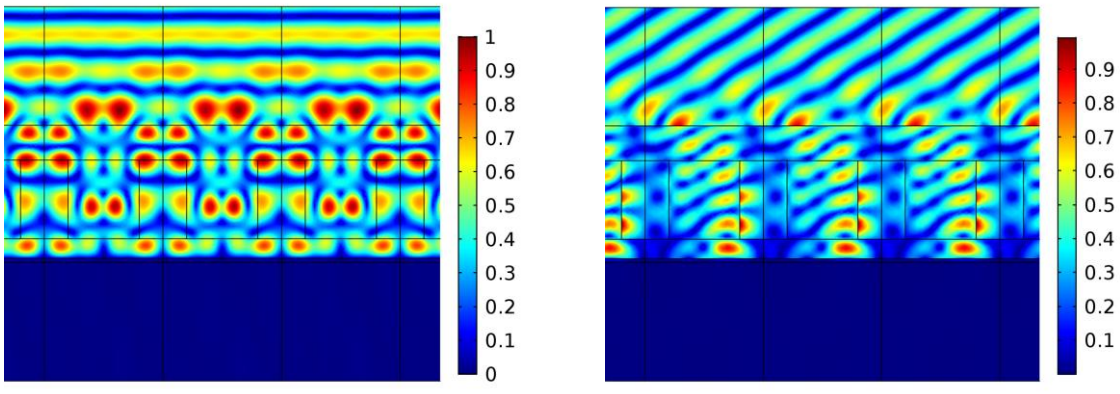

Fig. 3. Normalized field magnitude distribution with reflective polarization splitter under second Bragg angle incidence: (a) 0th order under TE polarization (b) -2nd order under TM polarization (color online)

3. Analysis and discussions

The wavelength of the polarization-reflecting beam-splitting grating can be studied by using rigorous coupled wave. Since the incident wavelength may vary around the central value in actual conditions, the reflection effect of the beam splitting grating is also different. Fig. 4 shows the relationship between the reflection efficiency or the extinction ratio of the grating and the incident wavelength. If the range of wavelength is 1547-1554 nm, the efficiency of the 0th order of the grating under TE polarization is greater than 95%, and the efficiency of the -2nd order under TM polarization is greater than 95%. If the incident wavelength is 1547-1554 nm, extinction ratios of the two orders are greater than 20 dB. Similarly, the difference in incident angle also affects the reflection efficiency of the device. Fig. 5 reflects the effect of different angles of incidence on the reflection efficiency and extinction ratio. If the incident angle is in the range of 31.0-32.1°, the efficiency of 0th order under TE polarization of the grating is greater than 95%, and the efficiency of the -2nd order under TM polarization is also greater than 95%. Extinction ratios of two orders in two polarization are greater than 20 dB in the range of 30.6-32.3°.

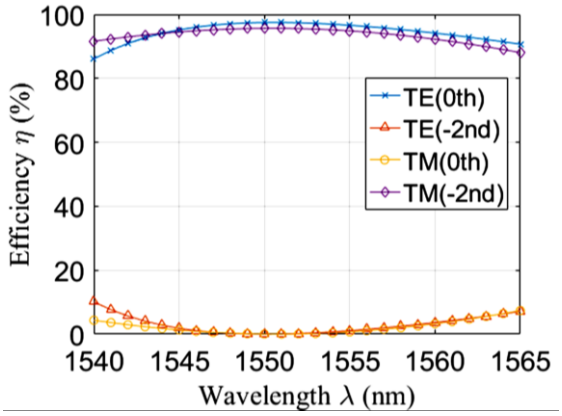

(a)

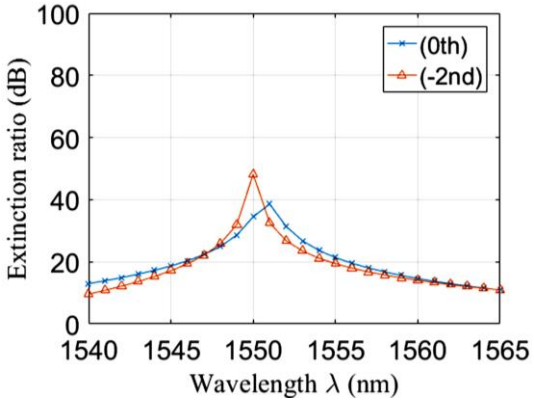

(b)

Fig. 4. (a) Reflection efficiency and (b) extinction ratio corresponding to the incident wavelength with f=0.6, d=2962 nm, h_1=0.87 μm, h_2=1.96 μm, and h_3=0.49 μm (color online)

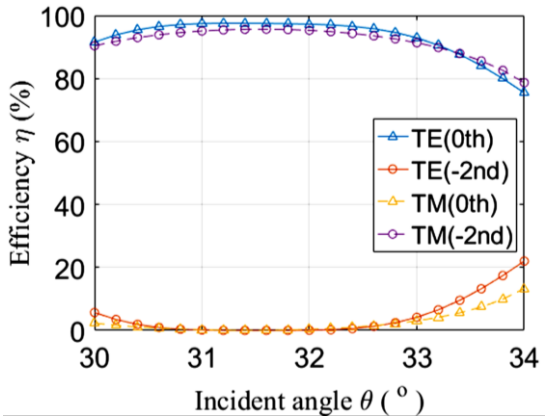

(a)

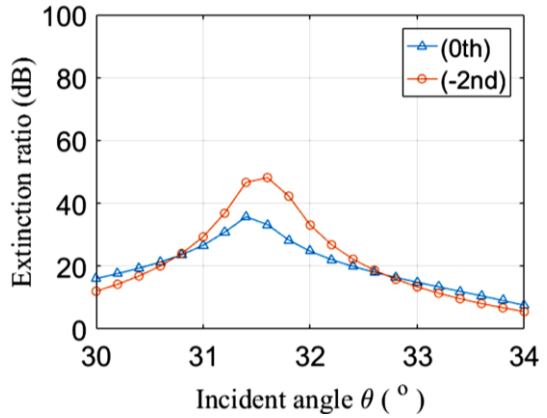

(b)

Fig. 5. (a) Reflection efficiency and (b) extinction ratio corresponding to the incident angle with f=0.6, d=2962 nm, h_1 = 0.87 μm, h_2 =1.96 μm, and h_3 =0.49 μm (color online)

Due to the impact of actual fabrication of micro-nano processing, the period or duty cycle of the grating may have some error during the manufacturing process. Therefore, the analysis of the process tolerance of the grating is required. Fig. 6 shows the relationship between the reflection efficiency and extinction ratio of the grating and the period. With the other grating structure parameters unchanged, when the period is in the range of 2941-2976 nm, the 0th order efficiency under TE polarization is greater than 95%, and the efficiency under TM polarization is greater than 95%. Extinction ratios of the two orders of are greater than 20 dB in the period range of 2950-2971 nm. Fig. 7 shows the relationship between efficiency of the grating or extinction ratio and duty cycle. If the duty cycle is changed in the range of 0.589-0.610, the 0th-order efficiency under TE polarization is greater than 95%, and the efficiency under TM polarization is greater than 95%. Extinction ratios of the two orders of are greater than 20 dB in the duty cycle range of 0.591-0.607.

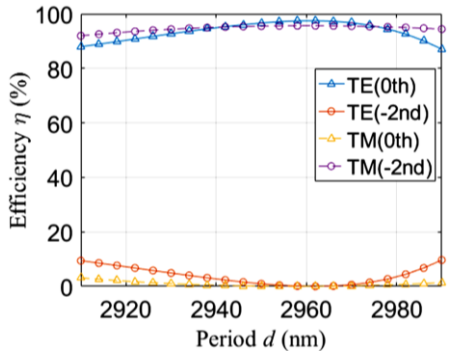

(a)

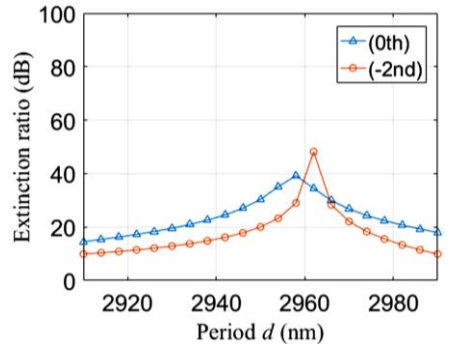

(b)

Fig. 6. Performance corresponding to the period with f=0.6, h_1=0.87 μm, h_2=1.96 μm, and h_3=0.49 μm: (a) reflection efficiency and (b) extinction ratio (color online)

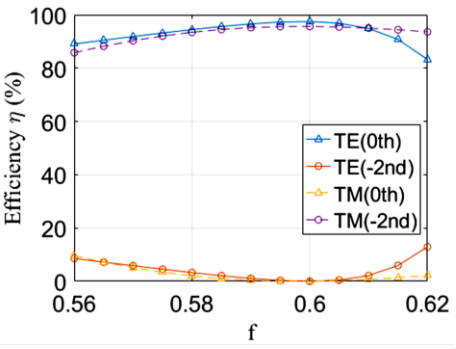

(a)

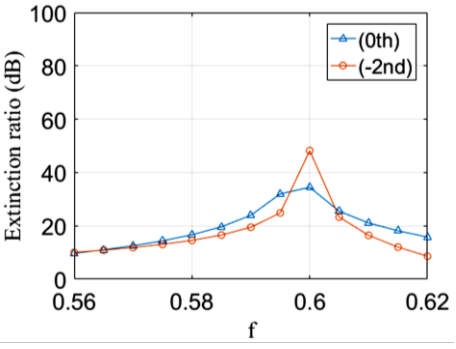

(b)

Fig. 7. Performance corresponding to the duty cycle with d=2962 nm, h_1=0.87 μm, h_2=1.96 μm, and h_3=0.49 μm: (a) reflection efficiency and (b) extinction ratio (color online)

4. Conclusion

In this paper, a polarization-dependent beam splitting grating under second Bragg incidence is presented based on reflection sandwich-type structure. The grating introduces a covering layer with low loss of incident light and stable performance. The optimized results show that the efficiency of the 0th order under TE polarization is 97.49%, and the efficiency under TM polarization is 95.65%. In the wavelength range of 1547-1554 nm or the range of 31.0-32.1°, efficiencies of the two orders are greater than 95%. Most importantly, extinction ratios are greater than 20 dB, which can achieve a good reflection beam splitting effect. The polarization-independent grating polarizer has a good application effect in the fields of laser and polarization imaging.

Acknowledgements

This work is supported by the Science and Technology Program of Guangzhou (202002030284, 202007010001, 202002030210) and the Science and Technology Planning Project of Guangdong Province (2020B090924001).

References

[1] B. Fang, S. Han, J. Xie, C. Li, Z. Hong, X. Jing, Optoelectron. Adv. Mat. **13**(3-4), 175 (2019).
[2] J. Wang, C. Liu, G. Wang, Y. Sun, Optik **182**, 1143 (2019).
[3] T. Sasaki, H. Kushida, M. Sakamoto, K. Noda, H. Okamoto, N. Kawatsuki, H. Ono, Opt. Commun. **431**, 63 (2019).
[4] H. Bencherif, L. Dehimi, F. Pezzimenti, F. G. Della Corte, Optik **182**, 682 (2019).
[5] H. Li, K. Wang, L. Qian, Optik **207**, 164432 (2020).
[6] X. Tong, B. Xu, M. Yan, Z. Sun, J. Zhou, K. Tian, T. E. Mupona, Optik **192**, 162981 (2019).
[7] P. Qiu, W. Pang, P. Fu, M. Li, C. Sun, J. Zhao, Y. Xie, Q. Kan, Optik **218**, 165125 (2020).
[8] L. Liu, Y. Li, X. Li, Opt. Commun. **458**, 124810 (2020).
[9] Y.-Z. Umul, Optik **179**, 135 (2019).
[10] J. Tian, J. Zhang, H. Peng, Y. Lei, L. Qin, Y. Ning, L. Wang, Optik **192**, 162918 (2019).
[11] D. Li, X. Wang, J. Ling, Y. Yuan, Opt. Commun. **445**, 90 (2019).
[12] H. Pang, A. Cao, W. Liu, L. Shi, Q. Deng, IEEE Photon. J. **11**(2), 1500909 (2019).
[13] Y. Chen, X. Zhang, W. Liu, Optik **218**, 165101 (2020).
[14] X. He, J. Jie, J. Yang, Y. Han, S. Zhang, Opt. Commun. **460**, 125145 (2020).
[15] K. Jin, W. Zheng, Y. Liu, C. Yang, J. Han, Y. Wang, H. Wang, Q. Liu, F. Huang, Optik **199**, 163352

(2019).
[16] C. Li, K. Zhang, Y. Zhang, Y. Cheng, W. Kong, Opt. Commun. **437**, 271 (2019).
[17] G. Zhang, X. Wu, Q. Ge, S. Li, D. Guang, S. Fang, C. Zuo, B. Yu, Opt. Commun. **448**, 64 (2019).
[18] W. Zhu, B. Wang, C. Fu, J. Fang, Laser Phys. **30**(6), 066201 (2020).
[19] J. Lou, T. Cheng, S. Li, Optik **179**, 128 (2019).
[20] H. Pei, B. Wang, J. Fang, C. Fu, K. Wen, Z. Meng, Z. Nie, X. Xing, L. Chen, L. Lei, J. Zhou, Optik **206**, 164361 (2020).
[21] S. S. M. Fard, A. H. Farhadian, M. Abbasabadi, Laser Phys. **30**(12), 126202 (2020).
[22] V. A. Reshetov, Laser Phys. **30**(8), 086001 (2020).
[23] M. V. Fedorov, Laser Phys. **29**(12), 124006 (2019).
[24] H. Wang, F. Zhao, Z. Yan, X. Hong, J. Song, K. Zhou, T. Zhang, W. Zhang, Y. Wang, Laser Phys. **29**(5), 055105 (2019).
[25] D. Meng, W. Lai, X. He, P. Ma, R. Su, P. Zhou, L. Yang, Laser Phys. **29**(3), 035103 (2019).
[26] B. Ibarra-Escamilla, M. Durán-Sánchez, R. I. Álvarez-Tamayo, B. Posada-Ramírez, E. A. Kuzin, S. Das, A. Dhar, M. Pal, M. C. Paul, A. V. Kiryanov, Laser Phys. **29**(1), 015102 (2019).
[27] K. Chen, M. Yi, F. Gao, X. Zhang, X. Yuan, IEEE Photon. Technol. Lett. **31**(10), 787 (2019).
[28] C. Fu, B. Wang, Laser Phys. **30**(7), 076205 (2020).
[29] L. Sun, R. Ni, H. Xia, T. Shao, J. Huang, X. Ye, X. Jiang, L. Cao, IEEE Photon. J. **10**(5), 8300115 (2018).
[30] W. Liao, X. Nie, Z. Liu, X. Nie, W. Wen, Optik **179**, 957 (2019).
[31] D. Kassegne, S. Singh, S.-S. Ouro-Djobo, M.-B. Mao, J. Opt. Technol. **86**(3), 160 (2019).
[32] Q. Ma, C. Li, Y. Zhang, X. Dai, Z. Cao, Y. Liu, Y. Xiang, Opt. Commun. **448**, 60 (2019).
[33] M. Jiang, Y. Chen, N. Cheng, Y. Sun, J. Wang, R. Wu, F. Yang, H. Cai, Y. Gui, IEEE Photon. J. **11**(3), 7202808 (2019).
[34] Q. Wu, Z. Feng, M. Tang, X. Li, M. Luo, H. Zhou, S. Fu, D. Liu, Sci. Rep. **8**, 15827 (2018).
[35] J. Zheng, C. Zhou, J. Feng, H. Cao, P. Lu, J. Opt. A **11**(1), 015710 (2009).
[36] B. Wang, L. Chen, L. Lei, J. Zhou, Opt. Commun. **296**, 149 (2013).
[37] M. G. Moharam, D. A. Pommet, E. B. Grann, T. K. Gaylord, J. Opt. Soc. Am. A **12**(5), 1077 (1995).
[38] I. C. Botten, M. S. Craig, R. C. Mcphedran, J. L. Adams, J. R. Andrewartha, Opt. Acta **28**(3), 413 (1981).

*Corresponding author: wangb_wsx@yeah.net